# Highlights

**Techno-economical modeling of a power-to-gas system for plant configuration evaluation in a local context**

Corey Duncan, Robin Roche, Samir Jemei, Marie-Cecile Pera

- Holistic power-to-gas modeling methodology for project techno-economical analysis is presented.
- Scenarios based upon different configurations and electricity cost structures analysed for a pilot project in Europe.
- Best scenarios include synthetic natural gas grid injection and mobility.
- Minimum selling price found to be significantly higher than current natural gas prices.
- Sensitivity analysis shows electrolyser efficiency and electricity price most influential.

# Techno-economical modeling of a power-to-gas system for plant configuration evaluation in a local context

Corey Duncan[a,*], Robin Roche[b], Samir Jemei[a], Marie-Cecile Pera[a]

[a]*FEMTO-ST Institute, FCLAB, Univ. Bourgogne Franche-Comté, CNRS, Belfort, France*

[b]*FEMTO-ST Institute, FCLAB, Univ. Bourgogne Franche-Comté, UTBM, CNRS, Belfort, France*

**Abstract**

Decarbonization of the European energy networks is critical to meet Commission targets in the coming decades. The presented study aims to contribute to this by analysing one of the proposed solutions: power-to-gas. A techno-economic model is created for the purposes of evaluating specific projects on their feasibility in terms of local constraints and opportunities, using a current project as a template for model generation and analysing different possible configurations in 8 operational scenarios. Five metrics were used for scenario analysis: levelized cost of methane, minimum selling price, operational hours, hydrogen tank size and capital cost. The results from the analysis indicate that, in terms of the stated project, synthetic natural gas production and grid injection along with on-site mobility applications provide the best economical result. However, selling prices of synthetic natural gas obtained are one magnitude higher than current natural gas prices, in-

*Corresponding author

*Email addresses:* corey.duncan@univ-fcomte.fr (Corey Duncan), robin.roche@femto-st.fr (Robin Roche), samir.jemei@femto-st.fr (Samir Jemei), marie-cecile.pera@femto-st.fr (Marie-Cecile Pera)

dicating government support is required for further development. Future projections of electrolyser efficiency and equipment capital costs will greatly reduce production costs, giving promise for feasible business cases in the coming years.
*Keywords:* power-to-gas, system modeling, techno-economical analysis, synthetic natural gas

---

**Nomenclature**

**Abbreviations**

BOP balance of plant

CNG compressed natural gas

DA day-ahead

FCR frequency containment reserve

GHG greenhouse gas

LCOE levelized cost of energy

NG natural gas

OH operational hours

PEM polymer electrolyte membrane

PtG power-to-gas

PtX power-to-X

SNG synthetic natural gas

TSO transmission system operator

VRE variable renewable energy

WTP willingness to pay

**Parameters**

$c_{BOP}$ cost of BOP (% of CAPEX)

$c_{var,rea}$ cost of reactor nutrient (€/Nm$^3$)

$CAPEX$ total capital expenditure in year 0, including BOP (€)

$CAPEX_{equip}$ total capital expenditure in year 0 (€)

$cons_{grid,t}$ local NG grid consumption at time step $t$ (Nm$^3$/10min)

$f_n$ nominal electrical grid frequency (Hz)

$f_t$ electrical grid frequency at time step $t$ (Hz)

$K$ FCR gain (MW/Hz)

$k_a$ discount factor

$n$ project lifespan (years)

$OH_{x,max}$ maximum yearly operational hours for equipment $x$ (hours)

$OPEX$ total yearly operational expenditure (€)

$OPEX_{fix}$ total yearly fixed operational expenditure (€)

$P_{elect,min}/P_{elect,max}$ electrolyser minimum/maximum power rating (MW)

$p_{min,tank}/p_{r,tank}$ minimum/rated tank pressure (bar)

$P_{r,elect}$ electrolyser rated power (MW)

$Q_{H_2,rea,min}/q_{H_2,rea,max}$ reactor minimum/maximum $H_2$ consumption ($Nm^3$/10min)

$Q_{H_2,rea,t}$ reactor $H_2$ consumption at time step $t$ ($Nm^3$)

$r$ discount rate (%)

$rr_{rea}$ reactor ramping rate ($Nm^3$/10min)

$t$ current time step of simulation $\forall t \in m$

$v_{FCR}$ price value of FCR participation (€/MW/h)

$v_{H_2}$ price value of $H_2$ for mobility (€/kg)

$WTP_{det}$ pre-determined willingness to pay (€/MWh)

**Variables**

$C_{rep}$ total levelized cost of equipment replacement during the project lifespan (€)

$F$ total yearly cost of feedstocks

$OPEX_{var}$ total yearly variable operational expenditure (€)

$P_{elect,tot,t}$ total electrolyser power at time step $t$, including FCR participation (MW)

$P_{elect,t}$ electrolyser power at time step $t$ (MW)

$P_{FCR,t}$ electrolyser power adjustment when participating in the FCR (MW)

$p_{tank,t}$ tank pressure at time step $t$ (bar)

$Q_{CNG,r}$ rated SNG production used for CNG mobility ($Nm^3$)

$Q_{H_2,mob,t}$ $H_2$ production used for mobility at time step $t$ ($Nm^3$)

$Q_{H_2,mob}$ yearly $H_2$ production used for mobility ($Nm^3$)

$Q_{SNG}$ total yearly SNG production ($Nm^3$)

$R_{FCR}$ yearly revenue from FCR participation (€)

$R_{H_2}$ yearly revenue from $H_2$ mobility (€)

$sig_{FCR,t}$ signal of electrolyser participation in the FCR at time step $t$

LCOM levelized cost of methane (€/MWh)

MSP minimum selling price (€/MWh)

## 1. Introduction

The 2030 Climate and Energy Framework (CEF) for the European Union (EU) has translated Paris Agreement commitments to mandatory EU-wide targets, specifically: reducing greenhouse gas (GHG) emissions by 40% from 1990 levels and increasing the share of renewables in primary energy to 32.5% [1]. Achieving the CEF targets as well as meeting higher demands of electrical energy are fueling a large up-take of variable renewable energy (VRE), namely wind and solar. However, energy systems with high shares of VREs require flexibility due to the spatial and temporal imbalances of supply and demand, which can be provided by multiple approaches, each with unique economical and technical benefits [2].

One such approach is using energy storage technologies as a means to absorb surplus electricity, shifting its time of delivery for periods of greater demand. Pumped hydro power is currently the primary energy storage technology used for electricity, with massive facilities worldwide. Several emerging storage solutions involve power-to-X (PtX) technologies, with over 150 demonstration projects in Europe either planned, operational or completed [3]. PtX can be defined as electrical power conversion to other energy applications, such as: transportation fuels, heating, chemical feedstock to produce liquid fuels or other chemicals or re-converted to power. A diagram of possible PtX pathways is shown in Figure 1. As is shown, PtX allows integration of gas and electricity networks, which provides several benefits such as: further improving flexibility of the system to integrate VREs, short- to long-term energy storage capabilities [4] and helping to decarbonize sectors other than electricity. [5]. When coupled with local VREs, it has been shown to decrease curtailment and avoid additional electrical infrastructure costs by using already available gas grid installations [6]. The main concept of PtX – producing energy-rich gases such as hydrogen ($H_2$) and methane ($CH_4$) from renewable energy sources – is called power-to-gas (PtG).

The core conversion of PtG pathways is water electrolysis: electrical dissociation of water ($H_2O$) to $H_2$ and oxygen ($O_2$). The $H_2$ gas can be used for transportation, providing significant sector carbon emission reduction potential when compared to fossil fuels [7] as well as longer range and higher specific energy (when compressed to 350 or 700 bar) than batteries [8]. It can also be directly injected into the natural gas (NG) grid, with a volumetric capacity of 0.1%-12% depending upon the respective European country's standards [9]. PtG also includes the possibility of further processing $H_2$ by combining it with carbon to produce methane ($CH_4$) via the Sabatier process in methanation reactors. The most common $H_2$ conversion process done in PtX projects [10], $CH_4$ reactors can be classified as either biological or catalytic. Biological reactors produce $CH_4$ using organic matter, namely hydrogenotrophic methanogens, in a low pressure and temperature environment [5] whereas catalytic reactors use nickel-based catalyst using high pressure and temperature [11]. The choice of proper technology depends on the system requirements, with biological reactors allowing higher levels of impurities and catalytic reactors achieving higher production rates [5]. Carbon dioxide ($CO_2$) is increasingly used as the carbon source for $CH_4$ production due to: (1) high availability as a byproduct from industrial, waste treatment and biogas facilities; (2) the reduction of $CO_2$ in the atmosphere; and (3) its low cost of 0-100 €/ton [11]. The product $CH_4$ is also known as synthetic natural gas (SNG) as it can be directly injected into the NG grid due to its similar physical properties, allowing the over 1,000 TWh European NG network capacity to be used for transmission, distribution and storage of the product gas [12]. In addition to the plethora of PtG production end-uses, it is also viewed as a technology capable of providing electricity grid ancillary services, ensuring grid stability in short (seconds) to long (months) durations [13].

Further development of the technologies involved in PtG as well as scaling

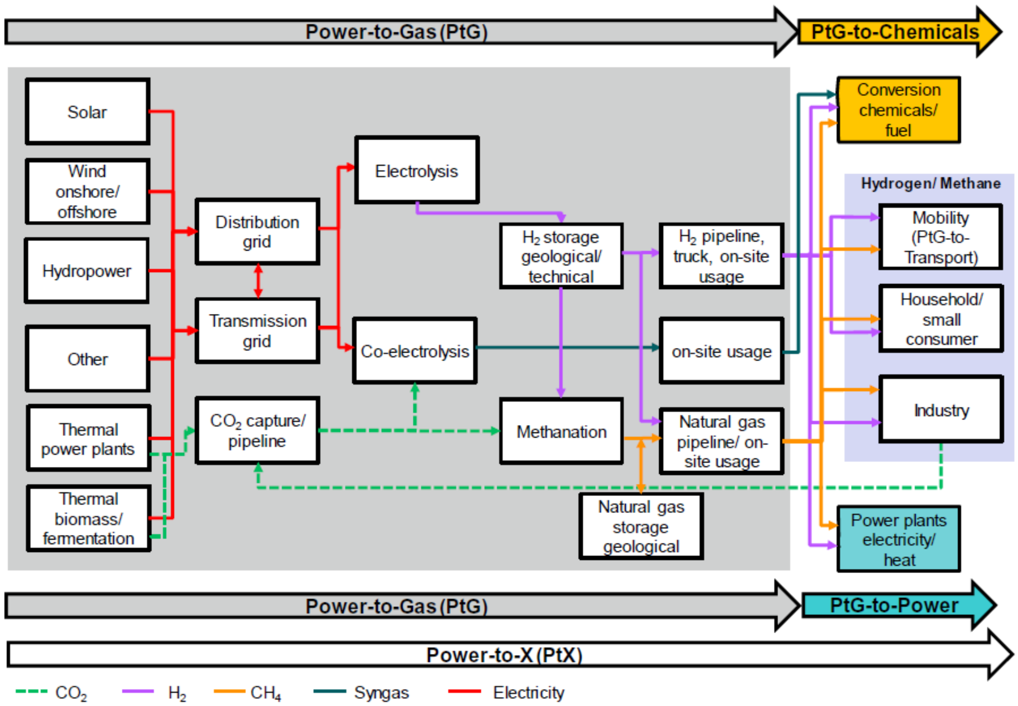


Figure 1: Overview of power-to-X pathways; source [14].

up are required to improve its economics. Götz et al. [11] and van Leeuwen and Zauner [15] concluded that high investment and electricity costs are the primary reasons for poor economics, with high yearly operational hours (OH) needed to reduce their effect. The inevitable high cost of the equipment can be attributed to the novelty of the technologies, namely (other than alkaline) electrolysis and methanation [16]. Nonetheless, PtG installed capacity has been exponentially increasing since the early 2000's as their costs continue to fall and business cases become realized [3]. De Bucy et al. [17] assessed the economical potential of PtG in Europe, concluding that mobility is the best current market with high OH and low electricity prices. Further, they found that the levelized cost of $H_2$ and SNG for grid injection were 5 and 8.5 times the current selling price of NG, respectively, and SNG costs 1.5-3 times higher than bio-NG, highlighting the need for regulatory incentives for commercial deployment. McDonagh et al. [18] studied SNG production as a transport fuel, calculating a cost of 107-143 €/MWh in 2020 when assuming an average electricity price of 35 €/MWh and 6,500 OH. They also showed the impact of several incentives schemes that could help lower the cost below NG, such as selling produced $O_2$ and grid services. However, this study focuses on a national level (Ireland) and does not discuss cost reduction strategies for individual plants. Flexible plant operation has been found to be economically preferred – operating the system when electricity prices are favorable versus continuous operation – with more than one revenue stream harnessed. Breyer et al. [19] modeled a PtG plant used on-site of a pulp mill in Finland with frequency containment reserve (FCR) market participation and 4,000 OH and found the business case to be profitable, with grid services representing 40% of total income. Bio-diesel and SNG produced were either used on-site or sold for mobility purposes. However, this model used an assumed fixed electricity price of 40 €/MWh, neglecting actual dynamic day-ahead (DA) electricity market participation. Limitations on local gas consumption were also not considered. Tractebel and Hinicio [20] designed three business case opportunities in Europe using local conditions with mobility and industry seen as the best current primary applications. DA market participation was considered, with a yearly average price below 40-50 €/MWh required to build a profitable business case. FCR participation was also found to reduce payback time by 30-50%, signifying its importance to profitability. However, the study only considered $H_2$ as a

PtG product, neglecting the potential of SNG and other byproducts. Gorre et al. [21] performed an optimization analysis of production costs of SNG in terms of various electricity purchasing and gas selling strategies for a PtG plant in 2030 and 2050, comparing them to the expected SNG prices. The results showed that flexible operation in DA markets with an average price of 30 €/MWh and 4,000 OH can have a positive revenue by 2050. However, the study is generic to Europe and does not consider participation in ancillary services, local technical or physical limitations, governmental support schemes or specific country DA electricity prices. From this literature review it is seen that most studies perform European-wide analyses suggesting broad action without considering local limitations or advantages, such as regional end-use applications, local restrictions in energy networks (namely NG and electricity networks for purposes of this paper) and DA energy prices. These parameters can and ultimately determine the viability of projects and allow a thorough investigation of local business case opportunities.

The scientific contribution of this paper is to present a methodology for performing a feasibility study of a PtG plant which focuses on analysing local conditions which effect operation, namely: variable electrical power source, DA variable and fixed electricity prices, possible local end-use applications and local gas grid injection limitations. Individually, these parameters can have profound implications on operational strategy; together they can completely change the plant's operational objective and its feasibility by giving a more complete picture of it's unique conditions. This methodology is applied to a pilot project currently underway in the form of a case study. Although the specific model created for this case study cannot be used for other projects as they all will have unique local conditions, it is believed that the methodology presented can be easily applied to similar projects, providing a thorough analysis of project feasibility. Further, an innovative electrolyser design is investigated that allows maximum capacity to be 200% rated for short durations. This can allow participation in ancillary services while not sacrificing on lost production due to reserved power or over-sizing the electrolyser for such service. As previously mentioned, high investment and electricity costs will present a major challenge in finding an optimal operational configuration that is profitable. To overcome this challenge, an analysis of the most influential economical factors will be done, highlighting what needs to be done to make a similar project feasible.

The objectives of this paper are to:

- Present a techno-economical model methodology for PtG plant analysis using local limitations and opportunities as operating constraints and several metrics for thorough analysis.
- Present the pilot project that will be used as a case study of model methodology application.
- Develop operational scenarios based off of local conditions for the pilot project and perform a feasibility study.
- Perform a sensitivity analysis on the most favorable scenarios to determine most influential factors on the results.

## 2. Methodology

### *2.1. Standard Configuration of Pilot Plant*

To develop the model, a current PtG project in which the authors are involved in named HYCAUNAIS is used. Located in Saint-Florentin, France the project is being led by Storengy and has several industrial and public partners, with secured funding from PIA ADEME, Bourgogne France-Comté region (FRI), FEDER and project partners [22]. As the project is based in France, regulatory and market conditions there will be used henceforth. It must be emphasized that the work performed for this paper is researched-based and not representative of actual project objectives of HYCAUNAIS - it is meant to analyse several possible scenarios which are based upon the project topology.

A diagram of the HYCAUNAIS plant layout and possible configurations is shown in Figure 2. The plant will produce low-carbon gas for NG grid injection and possibly mobility. Following the combined power production signal of two existing wind farms (1) provided by the wind farm operator and sourcing the electricity via a grid connection (2), a 1 $MW_{el}$ PEM electrolyser (3) will produce hydrogen for a 50 $Nm^3/h$ biological methanation reactor (4), with intermediate $H_2$ storage (5) installed between the electrolyser and reactor. Currently, gas from the landfill (6) on-site is being upgraded by a WAGABOX® unit (7). The technology, supplied by Waga Energy [23], combines membrane filtration and cryogenic distillation to filter 98 vol% pure bio-$CH_4$ from landfill gas ($CH_4$ from a landfill is considered biological as per French regulation [24] and international agencies such as the IEA [25]), recovering 90 vol% of the bio-$CH_4$ contained in it. This highly pure bio-$CH_4$

is being injected into the NG grid (8). The $CO_2$ stream (including some impurities) normally vented during membrane distillation will be utilized as the carbon source for methanation, which must be purified (9) prior to injection into the biological reactor. Intermediate storage of $CO_2$ (10) between the reactor and purifier is also used. Bio-NG captured during purification is combined with the produced SNG and injected into the NG grid at the same existing site used by the WAGABOX® unit. The project boundary is input from the electrical grid and WAGABOX® effluent to output to NG grid injection as shown in Figure 2. Normal cubic metres ($Nm^3$) are used throughout the article to represent gas volumes in a simple, comparative fashion. The configuration as described above is known as the standard configuration in this article. Mobility options and NG grid injection capacity improvement were also investigated and will be discussed in the next subsection.

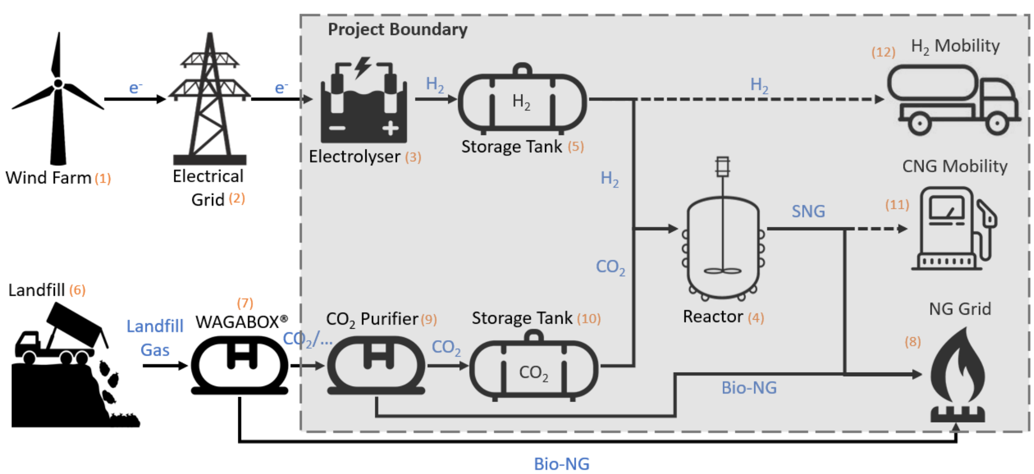


Figure 2: HYCAUNAIS project plant schematic and process flow.

To improve economics of the plant, participation in electricity grid services by the electrolyser is considered in all scenarios simulated, namely the primary reserve or FCR. Electrolysers have been shown to be capable of operating dynamically at ramping rates faster than required for FCR participation [26]. FCR consumer participation is compensated according to the reserve capacity in €/MW.30min in a market-based scheme, with participation given in 4-hour continuous blocks. More information on ancillary services are provided in [27]. Guinot et al. [28] concluded that an electrolyser participating in the FCR in France was not economical with the technical and economical assumptions made and current compensation values. However, as stated earlier, this study will investigate the use of an innovative electrolyser stack that is capable of doubling its rated capacity for periods longer than required for maximum frequency disturbance (15 minutes). This will allow the operator to offer the rated capacity of the electrolyser to the FCR while still operating at rated capacity, avoiding loss of hydrogen production for dedicated capacity on reserve for FCR solicitation.

### *2.2. Additional Configurations*

When injecting in the NG grid, knowledge of local capacity availability should be known as injection may not be possible all year round. If it is not, other end-use applications can be investigated to maximize the operational hours of the plant. NG grid expansion, increasing the local capacity, is also a possibility if the transmission systems operator (TSO) is interested in doing so. One specific scenario is called a "mesh upgrade" and includes installing a new pipeline between the local NG distribution grid and another grid in close proximity, essentially connecting two "island" distribution grids and consequently increasing both their capacities. This will be investigated as a possible plant "configuration": although the equipment will be the same as the standard configuration, the constraint of NG grid injection will be less stringent but still applicable, allowing for more injection throughout the year.

As seen in Figure 2, two mobility options are considered as additional end-use applications: $H_2$ and compressed natural gas (CNG). The mobility options must be designed for local transportation requirements to provide realistic approximation of their demand in the model simulation. Each mobility option will be evaluated separately as additional end-use applications to the standard configuration, increasing utilization of the plant.

### *2.3. Electricity Purchasing Contracts*

Two electricity purchasing contracts were investigated: long-term fixed-priced contracts or short-term DA market purchasing. Long-term contracts allow for operation of the plant at a specified fixed electricity price whereas DA market purchasing allow plant operators to take advantage of lower prices, choosing to operate when electricity prices are satisfactory as per conditions set by them.

### *2.4. Equipment Description*

#### *2.4.1. Electrolyser*

A 1 MW PEM electrolyser is used for the system and its modeling parameters are shown in Table 1. Values of parameters were either taken from sources listed or the HYCAUNAIS project directly. The investment cost or CAPEX listed only includes the cost of the electrolyser. Balance of plant (BOP) components (pumps, water purification, electronics, etc.) are included as a general BOP cost to the whole plant configuration of the scenario as shown in Equation 8. The electrical energy consumption of the electrolyser is represented as a range due to its variability in its operating range. The electrolyser is assumed to be capable of responding instantaneously to changes in power consumption, so ramping is not considered. Further, as mentioned earlier, an electrolyser capable of operating up to 200% its nominal capacity is considered. All values provided by the HYCAUNAIS project and its partners are shown under Source as "project".

Table 1: PEM electrolyser model parameters.

| **Parameter** | **Unit** | **Value** | **Source** |
|---|---|---|---|
| Rated power | $MW_{el}$ | 1 | project |
| Operating pressure | bar | 30 | project |
| Electrical energy consumption | $kWh/Nm^3\ H_2$ | 4.6-5.1 | [11] |
| Operational range | % rated power | 10-200 | project |
| Stack life | hours | 60,000 | [15] |
| Water consumption | $L\ H_2O/Nm^3\ H_2$ | 2 | [29] |
| CAPEX | € | 1,400,000 | [15] |
| Fixed OPEX | % CAPEX/a | 2 | [15] |
| Stack replacement cost | % CAPEX | 25 | [15] |

### *2.4.2. Methanation Reactor*

A biological reactor capable of consuming the rated flow rate of the electrolyser is used – 50 $Nm^3/h$. The model parameters used are shown in Table 2. Reactor electrical consumption is due to the continuous mixing from its internal propeller [30] which is assumed to be fixed when operational. Unlike electrolysers, methanation reactors have not been shown to be capable of operating at sufficient ramping rates while still maintaining high gas quality [31]. Thus, the model considers reactor ramping when changes in gas flow rates occur. Additionally, the reactor is assumed to be fed the methanation stoichiometric ratio of $H_2/CO_2 = 4$ at all times and a fixed $CO_2$ conversion rate occurring inside the reactor of 98 vol% (which has been shown to be possible with transient operation [32] and applied in other studies [21]). The fixed $CO_2$ conversion rate and $H_2/O_2$ ratio is applied throughout the reactor operational range, eliminating the requirement of modelling reactor kinetics.

Table 2: Biological methanation reactor model parameters.

| **Parameter** | **Unit** | **Value** | **Source** |
|---|---|---|---|
| Rated SNG capacity | $Nm^3/h$ | 50 | project |
| Inlet pressure | bar | 16 | project |
| Electrical energy consumption | $kWh/Nm^3$ SNG | 1 | [11] |
| CAPEX | € | 817,500 | [15] |
| Fixed OPEX | % CAPEX/a | 5 | [15] |

### *2.4.3. Carbon Dioxide Purification*

The $CO_2$ purification technology used is chemical scrubbing via amines due to its low pressure requirement and market availability [33]. However, it requires a heat source; it is considered to be harnessed from the reactor's exothermic heat dissipation. Model parameters used for chemical scrubbing are shown in Table 3. 4% of the biogas input is bio-NG - which can be captured and mixed with the produced SNG - and 88% is $CO_2$. The chemical scrubbing system is sized such that it is capable of purifying the rated $CO_2$ capacity of the reactor.

Table 3: $CO_2$ purification model parameters.

| **Parameter** | **Unit** | **Value** | **Source** |
|---|---|---|---|
| Electrical energy consumption | kWh/Nm$^3$ biogas | 0.15 | [34] |
| Water consumption | L $H_2O$/Nm$^3$ biogas | 0.032 | [33] |
| CAPEX | € | 91,200 | [33] |
| Fixed OPEX | % CAPEX/a | 3 | [33] |

### *2.4.4. Hydrogen Mobility*

$H_2$ mobility was designed as a refilling site for tube-trailers as there is no hydrogen consumption anticipated on-site. These trailers are able to travel up to 400 km from the fill-site to refuelling stations in local regions. Some of these regions, such as Bourgogne-Franche-Comté, are planning to enlarge their fuel cell electric vehicle (FCEV) bus fleets in the coming years [35]. The distributors in these regions are assumed to be the $H_2$ mobility consumers. Two tube-trailers with a capacity of 400 kg each at 200 bar were used, with an assumption that at least one will be available on-site to be filled at any time. The refilling station cost was calculated using a modeled developed by [20]. $H_2$ mobility model parameters are shown in Table 4. The refilling site was sized to be capable of receiving the rated capacity of the electrolyser.

Table 4: $H_2$ mobility model parameters.

| Parameter | Unit | Value | Source |
|---|---|---|---|
| Tube-trailer CAPEX | €/kg | 500 | [20] |
| Tube-trailer fixed OPEX | % CAPEX/a | 2 | [20] |
| Site CAPEX | € | 232,709 | [20] |
| Site fixed OPEX | % CAPEX/a | 3 | [20] |

### *2.4.5. Compressed Natural Gas Mobility*

A refuelling station was assumed to be installed on-site for CNG mobility which could be consumed by waste trucks used for landfill community pickup. It is proposed that the fleet could be switched to operate on CNG, starting with two trucks and possibly increasing in later years. However, the model simulation will only assume two vehicles for the project lifespan. The trucks are assumed to be filled overnight. The station is sized so that it can accept the rated capacity of the reactor if NG grid injection is not possible. The resulting refuelling station costs are shown in Table 5. Waste trucks are not included in the cost of the station. Costs were taken from values and models given in [36], which include a dispenser, time-fill post and gas dryer. Compressor cost is also included in the station CAPEX.

### *2.4.6. Gas Storage*

All tanks used in the system use the same CAPEX and OPEX parameters as listed in Table 6. The gas compressor parameters are also listed

Table 5: CNG mobility model parameters.

| Parameter | Unit | Value | Source |
|---|---|---|---|
| Station CAPEX | € | 232,417 | [36] |
| Station fixed OPEX | % CAPEX/a | 3 | [36] |

in this table. Intermediate $H_2$ storage is done at the equivalent pressure of electrolyser output, 30 bar, eliminating the need of a compressor. However, a compressor is required if $H_2$ mobility is considered for the tube-trailers, as described below. Intermediate $CO_2$ is pressurized to 16 bar to meet reactor input requirements while the $CH_4$ storage is at 200 bar for CNG mobility requirements. All tanks are assumed to have their complete capacity available for production. The electrical consumption varies greatly due to the pressure and gas being compressed [37]. The CAPEX of a compressor also varies greatly depending on the gas and compressor type; values for $H_2$ [20], $CH_4$ [38] and $CO_2$ [36] were taken from their respective source. The compressor must be completely replaced at the end of their useful life, which is defined as 10 years of continuous operation [15].

*2.4.7. Natural Gas Grid Injection*

The costs associated to NG grid injection are shown in Table 7. The difference in CAPEX values is due to the increased cost for installation of the mesh pipeline to connect two distribution grids.

Table 6: Gas tank and compressor model parameters.

| Parameter | Unit | Value | | | Source |
|---|---|---|---|---|---|
| | | $H_2$ | $CO_2$ | $CH_4$ | |
| Tank capacity | $Nm^3$ | see 3.4.4 | 50 | 600 | project |
| Tank rated pressure | bar | 30 | 16 | 200 | project |
| Tank CAPEX | €/$Nm^3$ | 100 | 100 | 100 | [15] |
| Tank fixed OPEX | % CAPEX/a | 2 | 2 | 2 | [15] |
| Compressor electrical consumption | kWh/kg | 1.68 | 0.09 | 0.20 | [37] |
| Compressor lifespan | hours | 87,600 | 87,600 | 87,600 | [15] |
| Compressor CAPEX | € | 200,000 | 234,636 | 101,398 | [20, 38, 36] |
| Compressor fixed OPEX | % CAPEX/a | 3 | 3 | 3 | [15] |
| Compressor replacement cost | % CAPEX | 100 | 100 | 100 | [15] |

Table 7: NG grid injection model parameters.

| Parameter | Unit | Value | Source |
|---|---|---|---|
| Grid injection CAPEX (no mesh) | € | 20,500 | project |
| Grid injection CAPEX (mesh) | € | 252,100 | project |
| Grid injection fixed OPEX | % CAPEX/a | 8 | [15] |

### *2.5. Operational Scenarios*

Eight scenarios were developed to evaluate the different plant configurations and electricity contracts. They are listed in Table 8, with the configuration and electricity purchasing option used marked accordingly. A "standard" configuration (S1 and S5) includes SNG production for NG grid injection only. The mesh upgrade scenarios (S2 and S6) increase the NG grid capacity by installing a new pipeline to connect two "island" distribution grids together whereas the mobility options (S2, S3, S6 and S7) use the standard configuration plus $H_2$ or CNG mobility stations. For $H_2$ mobility configurations, a refilling station with tube-trailers is used and consumption is only considered when SNG production is not possible. For CNG mobility configurations, a waste truck refuelling station on-site is considered which will have a continuous flow to fill the trucks daily, plus can also accept SNG production surplus when grid injection is not possible. Each configuration is tested independently to discover their individual attributes. Fixed electricity contract (S1-S4) and DA market participation (S5-S8) are also investigated for each configuration type to find what is the preferred electricity contract.

Table 8: Eight scenarios developed for project evaluation, with the type of electricity contract and configuration implemented in each scenario marked accordingly.

| **Scenario** | **Electricity Purchasing** | | **Configurations** | | | |
|---|---|---|---|---|---|---|
| | **Fixed Contract** | **DA Market** | **Standard** | **Mesh** | **$H_2$ Mobility** | **$CH_4$ Mobility** |
| S1 | X | | X | | | |
| S2 | X | | | X | | |
| S3 | X | | | | X | |
| S4 | X | | | | | X |
| S5 | | X | X | | | |
| S6 | | X | | X | | |
| S7 | | X | | | X | |
| S8 | | X | | | | X |

Table 9 shows the equipment considered for each scenario. As can be seen and was explained earlier, all scenarios consider SNG production and NG grid injection, with S2-S4 and S6-S8 also considering additional equipment to increase operational hours of the plant.

Table 9: The equipment considered for each scenarios configuration.

| **Equipment** | **S1** | **S2** | **S3** | **S4** | **S5** | **S6** | **S7** | **S8** |
|---|---|---|---|---|---|---|---|---|
| Electrolyser | X | X | X | X | X | X | X | X |
| $H_2$ tank | X | X | X | X | X | X | X | X |
| $CO_2$ purification | X | X | X | X | X | X | X | X |
| $CO_2$ compressor | X | X | X | X | X | X | X | X |
| $CO_2$ tank | X | X | X | X | X | X | X | X |
| Reactor | X | X | X | X | X | X | X | X |
| Grid injection | X | X | X | X | X | X | X | X |
| Grid injection w/ mesh | | X | | | | X | | |
| $H_2$ compressor | | | X | | | | X | |
| $H_2$ tube-trailer | | | X | | | | X | |
| $CH_4$ compressor | | | | X | | | | X |
| $CH_4$ tank | | | | X | | | | X |
| $CH_4$ fuelling station | | | | X | | | | X |

### *2.6. Analysis Metrics*

A multi-metric analysis was done to evaluate each operational scenario. Using the analysis results, users can determine what is the preferred configuration and electricity contract for their plant. Five metrics were analysed: levelized cost of methane (LCOM), CAPEX, minimum selling price (MSP), electrolyser OH and tank size. These metrics can be divided into economical and operational metrics, as described in the following subsections.

### 2.6.1. Economical Metrics

LCOM is a modified version of the levelized cost of energy (LCOE) which calculates the production cost of each unit of energy produced in the project lifespan in terms of the reference year and is a common way to compare energy costs of different technologies [11]. In this case, methane is being produced and the reference is the installation year (year 0). LCOM is found by using Equation 1:

$$LCOM = \frac{CAPEX + C_{rep} + (OPEX + F) \cdot k_a}{Q_{SNG} \cdot k_a} \tag{1}$$

where: $CAPEX$ is the capital expenditure of all equipment for the simulated scenario; $C_{rep}$ represents the total levelized cost of equipment replacement during the project lifespan; $OPEX$ is the operational expenditure of all equipment for the simulated scenario in the first year of operation (year 1); $F$ represents the costs of plant feedstocks, namely electricity and water in year 1; $Q_{SNG}$ is the total amount of SNG production in year 1 used for both CNG mobility and NG grid injection; $k_a$ is the discount factor, used to extrapolate all year 1 values over the whole project lifespan. It is calculated as shown in Equation 2 below:

$$k_a = \frac{(1 + r)^n - 1}{r(1 + r)^n} \tag{2}$$

where $r$ is the discount rate in % and $n$ is the project lifespan in years. $k_a$ is used to extrapolate values from year 1 over the project lifespan, which is then used in economical analysis. The values of $r$ and $n$ used are shown in Table 10. $OPEX$ can be broken down into two types of operational costs: fixed ($OPEX_{fix}$) and variable ($OPEX_{var}$) and are summed as shown in Equation

3:

$$OPEX = \sum_{t=1}^{m} OPEX_{var,t} + OPEX_{fix} \quad (3)$$

where $OPEX_{fix}$ represents the summed fixed operational costs of all equipment included in the simulated scenario, equal to a defined percentage of the equipment CAPEX. $OPEX_{var,t}$ represents the variable cost associated to operating the equipment at time step $t$ in the set $m$, representing the total number of time steps to simulate the calendar year. Only the reactor variable costs are considered in the simulation which is associated to nutrient replacement and can be found by multiplying the quantity of SNG produced at time step $t$ ($Q_{SNG,t}$) by a fixed cost of the nutrient ($c_{var,rea}$) as shown in Equation 4:

$$OPEX_{var,t} = Q_{SNG,t} \cdot c_{var,rea} \quad (4)$$

It should be noted that variable costs associated to feedstocks are considered separately. Further, when considering feedstock costs $F$ the electrical consumption of electrolysis, compressors, $CO_2$ separation and reactor mixing (continuously stirred tank reactor assumed to be used [30]) are included; electrolysis and $CO_2$ separation are considered for water consumption. For $C_{rep}$, the total number of operational hours determine when equipment must be replaced, with the replacement cost equal to a determined percentage of the CAPEX.

MSP is a metric used to include the revenue of FCR participation and $H_2$ sold for mobility purposes as a reduction of the LCOM to determine what is the minimum selling price SNG can be sold (in €/MWh) for either

CNG mobility or gas grid injection applications. MSP can be found by using Equation 5:

$$MSP = \frac{(OPEX + F - R_{H_2} - R_{FCR})k_a + CAPEX + C_{rep}}{Q_{SNG} \cdot k_a} \tag{5}$$

where $R_{H_2}$ and $R_{FCR}$ are the revenue from $H_2$ mobility and FCR, respectively, in year 1. It can be seen that besides the inclusion of these revenues the rest of the equation is identical to the LCOM equation. $R_{H_2}$ is found by Equation 6:

$$R_{H_2} = \sum_{t=1}^{m} Q_{H_2,mob,t} \cdot v_{H_2} \tag{6}$$

where $Q_{H_2,mob,t}$ is the quantity of $H_2$ used for mobility at time step $t$ and $v_{H_2}$ is the price value of hydrogen for mobility in €/kg. $R_{FCR,t}$ is generated only if the electrolyser is participating in the FCR during the time step $t$ as shown in Equation 7:

$$R_{FCR} = \sum_{t=1}^{m} sig_{FCR,t} \cdot v_{FCR} \cdot P_{r,elect} \tag{7}$$

where $sig_{FCR,t}$ is a signal indicating if the electrolyser is active in the FCR at time step $t$ ($sig_{FCR,t} = 1$ if participating and $sig_{FCR,t} = 0$ is not participating), $v_{FCR}$ is the price value of participating in the FCR in €/MW/h and $P_{r,elect}$ is the rated power of the electrolyser in MW.

$CAPEX$ is the total capital costs of all equipment in the simulated scenario multiplied by an additional balance of plant (BOP) cost - design, engineering, and other additional costs - as shown Equation 8:

$$CAPEX = CAPEX_{equip} \cdot (1 + c_{BOP}) \tag{8}$$

where $CAPEX_{equip}$ is the total CAPEX of all equipment included in the simulated scenario and $c_{BOP}$ is the BOP cost. Although CAPEX is included in the calculation of the other economical metrics, it is valuable to evaluate independently to appreciate the initial cost required for plant construction.

#### *2.6.2. Operational Metrics*

OH of the electrolyser or $\mathrm{OH_{elect}}$ is the total of partial, rated and overload operational hours of the electrolyser in the year. It is use as a metric gives insight into the effect OH has on the levelized cost and how much operation is required to obtain those costs.

Intermediate hydrogen tank size is determined independently from the main model for each scenario to give the lowest MSP. This will ensure that the tank is not oversized and increase the investment cost without any economical benefit. The resulting capacity will determine the duration of storage capable for the configuration: larger tanks can prolong production in times of unfavorable hydrogen production and allow continuous reactor operation; smaller tanks will require indeterminacy in reactor operation, more closely following electrolyser operation.

A scaled comparison of the key metrics in each scenario is helpful for analysis. Once scaled in a defined range $[a, b]$, the ranking of each scenario's metric value can be compared. This can be done by normalizing each scenario metric using Equation 9:

$$x_{i,n} = (b-a)\frac{x_i - min(x_i))}{max(x_i) - min(x_i)} + a \quad (9)$$

where: $x_i$ is equal to metric $i$'s value of each scenario; $x_{i,n}$ is the normalized value of metric $i$ in each scenario and $min(x_i)$ and $max(x_i)$ are the minimum and maximum scenario value of metric $i$. This equation will rank values such that the highest value in each metric receives the highest rank. If the lowest value of the metric should be ranked the highest, the equation must be slightly modified as in Equation 10:

$$x_{i,n} = (b-a)\left(1 - \frac{x_i - min(x_i))}{max(x_i) - min(x_i)}\right) + a \quad (10)$$

### *2.7. Model Constraints*

Constraints of model variables must be defined for model operation. $Q_{SNG,t}$ should not be higher than the current local NG grid consumption ($cons_{grid,t}$) for every iteration $t$ in the simulation. If it is, there is no capacity available for grid injection. This is shown in Equation 11:

$$Q_{SNG,t} \leq cons_{grid,t} \quad (11)$$

A maximum yearly operational hours must be defined for the electrolyser ($OH_{max,elect}$) and reactor ($OH_{max,rea}$) in the simulation to allow for maintenance. These constraints are shown in Equations 12 and 13:

$$OH_{elect} \leq OH_{max,elect} \quad (12)$$

$$OH_{rea} \leq OH_{max,rea} \quad (13)$$

where $OH_{elect}$ and $OH_{rea}$ are the total yearly operational hours of the electrolyser and reactor, respectively. The electrolyser and reactor must also operate within their allowable production limits. For the electrolyser this is defined by its electrical power consumption while the reactor is defined by its hydrogen consumption. This is shown in Equations 14 and 15:

$$P_{elect,min} \leq P_{elect,t} \leq P_{elect,max} \tag{14}$$

$$Q_{H_2,rea,min} \leq Q_{H_2,rea,t} \leq Q_{H_2,rea,max} \tag{15}$$

where $P_{elect,min}$ and $P_{elect,max}$ are the minimum and maximum operational power consumption of the electrolyser, respectively, and $P_{elect,t}$ is the operational power consumption at time step $t$. $Q_{H_2,rea,min}$ and $Q_{H_2,rea,max}$ are the minimum and maximum hydrogen consumption of the reactor, respectively, and $Q_{H_2,rea,t}$ is the hydrogen consumption of the reactor at time step $t$. The hydrogen tank pressure must be within its minimum and rated pressure, as shown in Equation 16:

$$p_{min,tank} \leq p_{tank,t} \leq p_{r,tank} \tag{16}$$

where: $p_{tank,t}$ is the hydrogen pressure in the tank at time step $t$; $p_{r,tank}$ is the rated pressure capacity and $p_{min,tank}$ is the minimum tank pressure. Ramping for the electrolyser was assumed to be instantaneous as explained in 2.1; the reactor could not be assumed to do so. Two different ramping rates were used for the reactor depending upon the hydrogen flow rate to the reactor: above or below rated capacity. This is expressed in the conditional Equation 17:

$$rr_{rea} = \begin{cases} rr_{rea,below}, & if\, Q_{H_2,rea,t} \leq Q_{r,H_2,rea} \\ rr_{rea,above}, & if\, Q_{H_2,rea,t} \geq Q_{r,H_2,rea} \end{cases} \tag{17}$$

where $rr_{rea,below}$ and $rr_{above}$ is the ramping rate below and above reactor rated capacity, respectively. The ramping rate values are sensitive to the project partner and thus cannot be listed. The electrolyser will ideally operate at rated power continuously for maximum production and reduced wear on the equipment. Further, as the profitability of the plant is the primary objective, participating in the FCR should be maximized. To be able to participate at 100% rated capacity, the electrolyser must be operating at rated capacity to offer a symmetrical reserve. Therefore, continuous operation of the electrolyser at rated capacity is desired, as long as other system limitations allow it. To keep the carbon intensity of the plant minimized, the plant is said to be following the wind profile whenever total power output from the wind farms is above rated capacity of the electrolyser; if not, it will purchase from other sources on the grid. As France's power generation is over 87% low-carbon and 22% renewable [39] as of 2019, the gases could still be considered "green" depending on the definition, but is certainly low-carbon. This consideration for power source is shown in Equation 18:

$$P_{elect,t} = \begin{cases} P_{wind,t}, & if\, P_{wind,t} \geq P_{r,elect} \\ P_{grid,t}, & else \end{cases} \tag{18}$$

where $P_{wind,t}$ is the the electrical power of the wind farm at time step $t$ and $P_{grid,t}$ is electrical power sourced from other grid sources. When considering DA market electricity prices (S5-S8), it is beneficial to operate only when electricity prices favor production. This can be defined as the willingness to pay (WTP) for electricity: if the electricity price is above a certain value, the operator of the plant will choose not to run production; if the price is below that value the plant will operate. In the short-term, this value would be determined by the marginal profit of the plant at each hour whereas in the long-term, total costs and revenues must also be considered [40]. For the purposes of the model, a range of electricity prices will be used to find the optimal WTP for plant operation in each scenario: if the variable cost of electricity at time step $t$ ($c_{el,t}$) is lower than or equal to the pre-determined WTP ($WTP_{det}$), the electrolyser will operate at the determined power level; if $WTP_{det}$ is larger than $c_{el,t}$, the electrolyser will sit idle. This is expressed in Equation 19:

$$P_{elect,t} = \begin{cases} P_{elect,t}, & if\, c_{el,t} \leq WTP_{det} \\ 0, & else \end{cases} \tag{19}$$

As electrolyser and reactor operation are decoupled due to intermediate hydrogen storage, the reactor may still be producing if the electrolyser is sitting idle: reactor operation depends on hydrogen availability in the storage tank and not hydrogen production. When participating in the FCR, the electrolyser power has a further constraint such that it must follow the frequency of the grid: when the frequency is below 50 Hz, less power must be consumed to bring it back to balance; when the frequency is above 50 Hz, more power must be consumed. This relationship can be expressed in Equations 20 and 21:

$$P_{FCR,t} = sig_{FCR,t} \cdot K(f_t - f_n) \tag{20}$$

$$P_{elect,tot,t} = P_{elect,t} + P_{FCR,t} \tag{21}$$

where $P_{FCR,t}$ power adjustment of the electrolyser at time step $t$ in MW; $K$ is the FCR gain as defined by the TSO (RTE) for the consumption site in MW/Hz [41]; $f_t$ is the measured grid frequency at time step $t$ in Hz; $f_n$ is the nominal grid frequency in Hz and $P_{elect,tot,t}$ is the total electrolyser power consumption at time step $t$. Note that $P_{FCR,t}$ can be negative or positive, depending on the grid frequency measured at that time step.

### *2.8. Operational Strategy*

Operational strategies when mobility is included as an extra end-use application is required. For $H_2$ mobility configurations, a refilling station with tube-trailers is used and consumption is only considered when SNG production is not possible. For CNG mobility configurations, a waste truck refuelling station on-site is considered which will have a continuous flow to fill the trucks daily, plus can also accept SNG production surplus when grid injection is not possible.

A continuous flow rate from the reactor to the refuelling station is assumed that is equal to the estimated yearly mileage and fuel efficiency of a CNG waste truck as proposed by [42] and shown in Equation 22:

$$Q_{CNG,r} = \frac{n_{trucks}(35Nm^3/100km)(20,000km/year)}{8760h} \tag{22}$$

where $Q_{CNG,r}$ is the hourly SNG production to the refuelling station and $n_{trucks}$ is the number of CNG waste trucks.

The constraints and assumptions presented above provide the framework for operation simulation. The model begins operation with variable input data and defined parameters, performing a loop of one year in defined time steps. Logic controllers determine the flow of model execution at each iteration, inputting the required data to modules representing the plant equipment. These equipment modules compute their production costs and resultant gas flow rates, inputting them into the next controller or to the final module for economical analysis.

The time step used for modeling is 10-minutes to equal the resolution of data given for the wind farm power profile for an entire year, equaling 52,560 time steps performed by the simulation. Further, a maximum operational time of 95% of the year was chosen for the electrolyser and reactor ($OH_{max,elect} = OH_{max,rea} = 8322$), allowing some hours during the year for operational maintenance.

### *2.9. Economical Parameters*

The economical parameters used for modeling are shown in Table 10. It was assumed that a fixed electricity contract of 65 €/MWh could be attained for the duration of the project. A local fixed water price is used for the model [43]. Enumeration for electrolysers in the FCR is based upon the DA market reserve price, with payment given to each MW for the bid duration. Historical data is provided by [44], given in €/MW/30min. Between 2016-2019, hourly prices have fluctuated between 4-20 €/MW/h, with the average in 2019 being 9 €/MW/h. The price of $H_2$ sold to distributors (refuelling stations) is taken from [20]. A discount rate of 7% and project lifespan of 20 years are used.

Table 10: Economical model parameters.

| Parameter | Unit | Value | Source |
|---|---|---|---|
| Fixed electricity price | €/MWh | 65 | project |
| Water cost | €/$m^3$ | 1.60 | [43] |
| BOP ($c_{BOP}$) | % CAPEX | 40 | [15] |
| FCR participation price | €/MW/h | 9 | [44] |
| $H_2$ selling price (distributor) | €/kg | 7 | [20] |
| Discount rate ($r$) | % | 7 | project |
| Project lifespan ($n$) | years | 20 | project |

### *2.10. Sensitivity Analysis*

A sensitivity analysis is performed to visualize the influence of various input values. The values chosen to be investigated are: electricity price, gas grid availability, electrolyser efficiency and electrolyser and reactor CAPEX. The sensitivity analysis is chosen to be done on the most favourable scenarios as chosen during the analysis of the key metrics.

## 3. Results and Discussion

An analysis of model inputs is done first to understand what limitations and opportunities they provide. This includes: electricity price, local gas consumption and wind power. The key parameters results for each scenario in 2017 and 2018 will then be analysed, determining the advantages and disadvantages of the configurations and where improvements are needed to give more favorable results.

### 3.1. Electricity Price Analysis

As electricity is the most costly part of power-to-gas operation, an analysis of DA market SPOT electricity prices over the year can give important operational insights. Figure 3a shows the average daily price variance over 2017 and 2018. A price duration curve - a curve showing the distribution of electricity prices by its frequency in the year - for 2017 and 2018 are shown in Figure 3b and include the taxes, fees, levies and wholesale price. The fixed price used is also represented as a horizontal line for reference. We can see the the average price of 2018 is roughly equal to the fixed price (64.8 €/MWh) while 2017 is lower at 59.57 €/MWh, suggesting lower operational costs are possible in the DA market but this can vary by year.

To determine how the variability of price will effect operational costs, 6 $\mathrm{WTP_{det}}$ values were tested: 55, 65, 75, 85, 95 and 105 €/MWh. Based upon these "cut-off" prices, the maximum amount of possible operational hours for the year (shown as the duration of the year) and the average electricity price for those available hours can be found. They are shown in Table 11. It can be seen that at 55-65 €/MWh, the duration of the year possible for operation varies greatly by year, but then converge at around 85 €/MWh. This suggests great variability by year in operation (27-71%) if lower $\mathrm{WTP_{det}}$ values are used, greatly influencing the production costs of the plant. Further, it can be seen that the average price is never higher than the fixed price used, meaning lower overall electricity prices when participating in the DA market. To determine the ideal $\mathrm{WTP_{det}}$, the scenarios were simulated with each $\mathrm{WTP_{det}}$ value to see their respective LCOM. The result for S5 in 2017 is shown in Figure 4 as well as the relationship to OH. As can be seen,

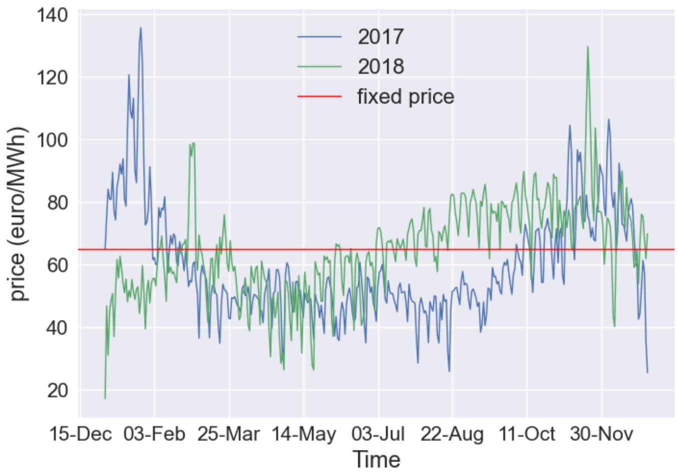


(a) Average DA market SPOT price over the year.

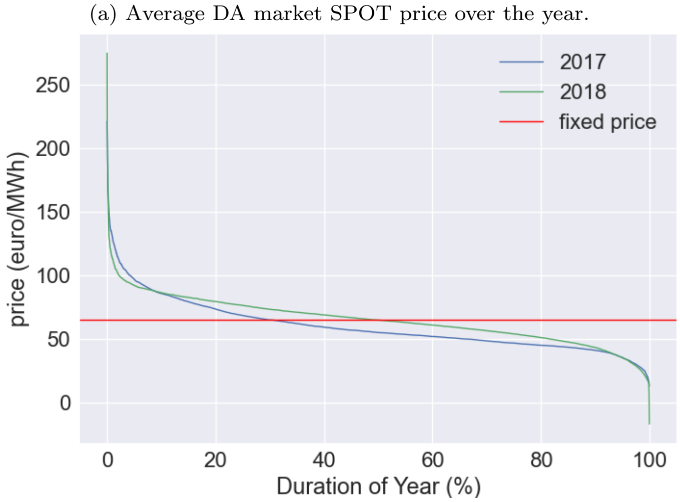


(b) SPOT price duration curve.

Figure 3: DA market SPOT price for 2017 and 2018 represented by its yearly distribution and duration of the year; the fixed price is also shown for reference.

the $WTP_{det}$ is very influential on operational costs at lower values, but has little impact past 85 €/MWh. All scenarios in both years have the same relationship as described above for S5. Therefore, a $WTP_{det}$ of 95 €/MWh was used for all DA electricity price scenarios (S5-S8) to minimize production costs and allow for the possibility of maximum yearly operational time (95%) during the simulation.

Table 11: The duration of year and average electricity price for each $WTP_{det}$.

| $WTP_{det}$ (€/MWh) | 2017 Duration of year (%) | 2017 Avg price (€/MWh) | 2018 Duration of year (%) | 2018 Avg price (€/MWh) |
|---|---|---|---|---|
| 55 | 50.64 | 45.37 | 27.58 | 43.67 |
| 65 | 70.61 | 49.39 | 51.54 | 51.4 |
| 75 | 81.47 | 52.06 | 73.40 | 56.86 |
| 85 | 89.55 | 54.56 | 88.88 | 60.87 |
| 95 | 94.60 | 56.42 | 96.46 | 63.01 |
| 105 | 96.94 | 57.47 | 98.50 | 63.84 |

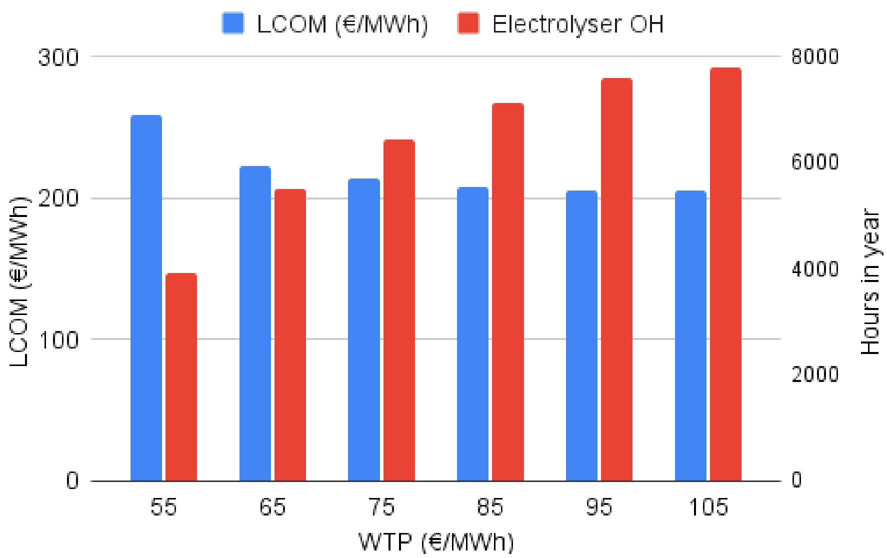


Figure 4: $WTP_{det}$ versus LCOM and electrolyser OH for S5 in 2017.

### 3.2. Gas Consumption Analysis

A study performed by the grid operator for the project revealed that SNG production could not be injected into the local grid year-round: at certain times of the year, namely summer months, there was not enough (close to zero) NG consumption to allow for grid capacity to be available for SNG injection. Local NG distribution network consumption determines the availability of gas grid capacity for SNG injection: as long as consumption is greater than SNG production, injection can take place. If not, the SNG must be used elsewhere, stored or not produced at all. This condition is very site-specific as consumption depends on many factors, such as: number of consumers, types of consumers, capacity of network, etc. If the duration curves are plotted for each year with and without the mesh and compared to the reactor rated capacity, as shown normalized in Figure 5, the amount of time in the year injection can take place is clearly seen: 86-88% without mesh and 94-98% with mesh. When a mesh upgrade is not installed, there will be many hours throughout the year where injection cannot take place, mainly in the summer months. This suggests additional end-use applications could be favorable to increase plant utilization, as long as their costs outweigh their benefits. It would be difficult to apply the same logic when the mesh upgrade is installed as there are very little hours in the year, if any, left to justify the additional investment.

### *3.3. Wind Power Analysis*

The wind farm power profiles are to be followed virtually by the electrolyser, via a connection to the grid. Data for two wind farms for a total capacity of 24 MW was provided by a project partner. The maximum amount of wind power utilization is desired to produce green hydrogen. Analysing the wind power profiles produced from the two wind farms in each year will give insights into how much of $H_2$ production can be produced from virtually

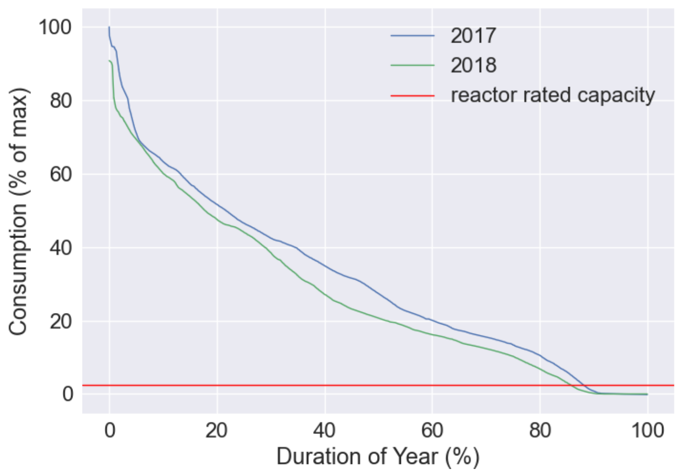


(a) Without mesh upgrade.

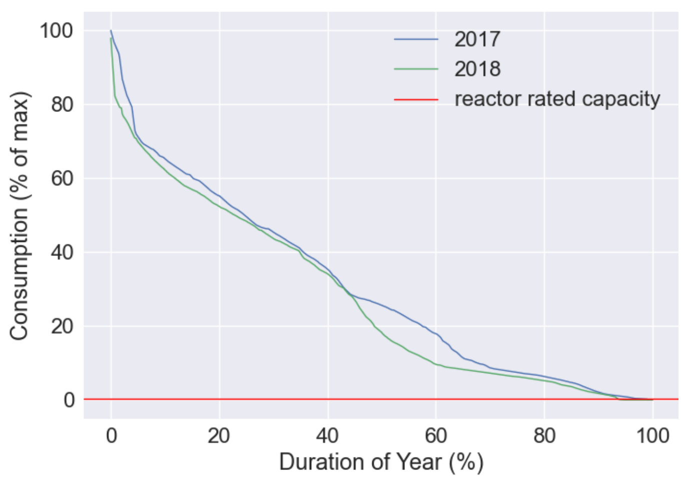


(b) With mesh upgrade.

Figure 5: Local NG network consumption normalized duration curve for 2017 and 2018 with and without the mesh upgrade; reactor rated capacity is also shown as a constant production.

following the wind power profile over the year, determining the "greenness" of the gas. Figure 6a shows the normalized average daily total wind power for 2017 and 2018. The high variability of wind power can easily be seen.

with lower production in the warmer months. Fortunately, the total rated capacity of the wind farms is significantly higher than the electrolyser rated capacity, allowing for majority of gas production to be done with renewable electricity. Indeed, the wind power exceeds electrolyser rated capacity for roughly 75% of the year in 2017 and 2018 as can be seen in normalized Figure 6b.

### *3.4. Results of Key Metrics*

The key metric results are shown in Table 12 for each scenario in 2017 and 2018. Each metric will be discussed independently in the following subsections.

Table 12: Key metric results for each scenario by year. The minimum values for LCOM, MSP and CAPEX are highlighted green and maximum highlighted red, as a lower value is desired. The maximum values in $OH_{elect}$ and tank size are highlighted green and minimum highlighted red, as a higher value is desired.

| Scenario | LCOM (€/MWh) | MSP (€/MWh) | $OH_{elect}$ (hours) | $H_2$ Tank Size ($Nm^3$) | CAPEX (€) |
|---|---|---|---|---|---|
| **2017** | | | | | |
| S1 | 213.19 | 183.24 | 8,031 | 215 | 3,411,242 |
| S2 | 218.07 | 188.28 | 8,322 | 130 | 3,723,582 |
| S3 | 262.25 | 204.73 | 8,322 | 50 | 4,553,934 |
| S4 | 216.67 | 186.91 | 8,322 | 50 | 3,721,956 |
| S5 | 205.60 | 175.79 | 7,587 | 325 | 3,426,642 |
| S6 | 204.38 | 174.60 | 8,264 | 175 | 3,729,882 |
| S7 | 247.15 | 189.47 | 8,275 | 120 | 4,563,734 |
| S8 | 202.67 | 172.91 | 8,287 | 120 | 3,731,756 |
| **2018** | | | | | |
| S1 | 213.33 | 183.36 | 8,035 | 215 | 3,411,242 |
| S2 | 218.95 | 189.06 | 8,322 | 130 | 3,723,582 |
| S3 | 268.16 | 204.62 | 8,322 | 50 | 4,553,934 |
| S4 | 216.62 | 186.88 | 8,322 | 50 | 3,721,956 |
| S5 | 213.24 | 183.35 | 7,767 | 325 | 3,426,642 |
| S6 | 218.79 | 188.97 | 8,052 | 175 | 3,729,882 |
| S7 | 264.87 | 201.31 | 8,322 | 120 | 4,563,734 |
| S8 | 214.27 | 184.48 | 8,303 | 120 | 3,731,756 |

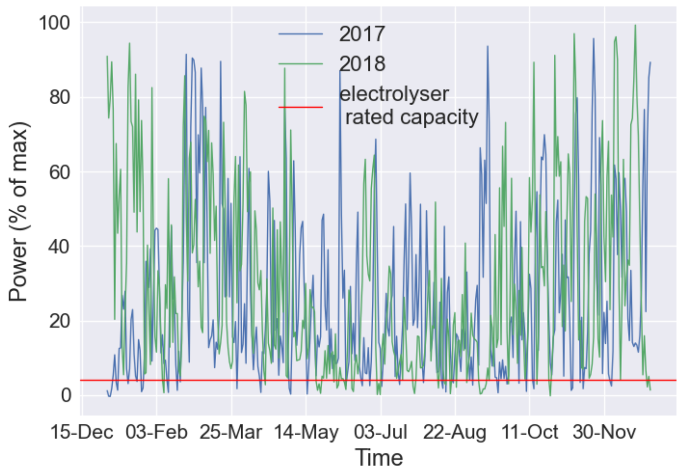


(a) Average daily total wind power over the year.

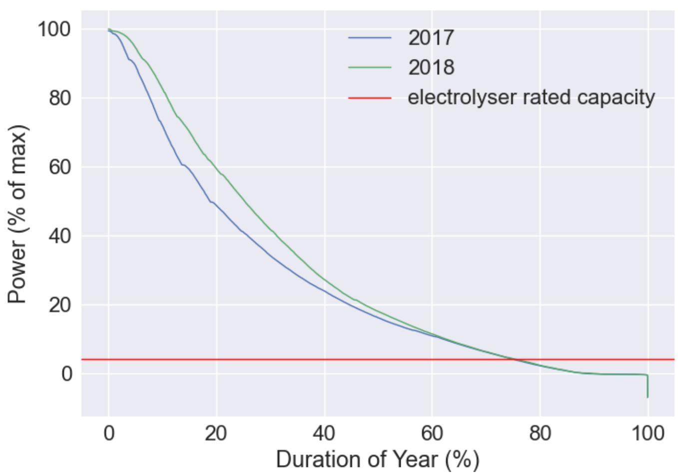


(b) Wind power duration curve.

Figure 6: Total wind power for 2017 and 2018 normalized and represented by its yearly distribution and duration of the year; electrolyser rated capacity is also shown as a constant production.

### *3.4.1. Levelized Cost of Methane*

The LCOM for fixed electricity price scenarios (S1-S4) for 2017 and 2018 are very similar, while DA pricing scenarios (S5-S8) can vary significantly by year, with S7 having the largest difference at 17 €/MWh. This relationship between the years is attributed to the difference in DA electricity prices, showing its impact on production costs. Figure 7 shows a breakdown of the LCOM by cost type and also by equipment or electricity type, with the top three contributors in each breakdown value shown. Fuel costs includes water and electricity as $CO_2$ is free in the project. As the water cost is almost negligible, fuel costs essentially represents the cost of electricity, which is 46-55% of the LCOM, depending on the scenario. Electricity cost is less in S5-S8, which is due to the lower average electricity price as described in section 3.1. The reason for such a high cost proportion for electricity is water electrolysis to produce $H_2$, which accounts for 43-51% of LCOM, depending on the scenario. The next highest costs by equipment are the electrolyser and reactor, respectively, due to their high CAPEX.

The lowest LCOM is CNG mobility with NG injection (S8) in 2017 and only NG injection (S5) in 2018, with both scenarios' LCOM similar in both years. This result suggests a tradeoff between these configurations: if more operational hours of the plant are desired and the additional upfront costs of CNG mobility can be attained, it is an attractive option. However, S6 also has a low LCOM in both years, suggesting the mesh upgrade investment can payoff. This may be preferred as increased gas grid injection has a lower risk in terms of offloading product gas as grid injection is guaranteed to be available – as long as local consumption allows it, which is almost always the case with the mesh upgrade – whereas gas sold for CNG mobility is dependent upon immediate local needs for transportation. Further, it can be seen that LCOM of S1 is comparatively low in 2018 to almost all the DA

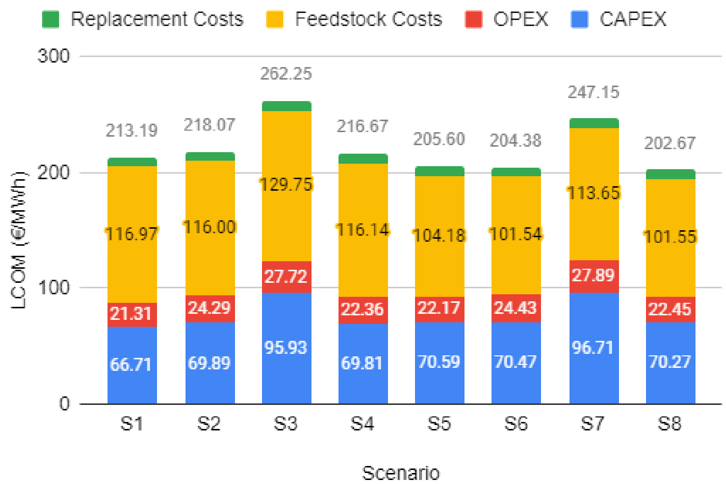


(a) LCOM grouped by cost type.

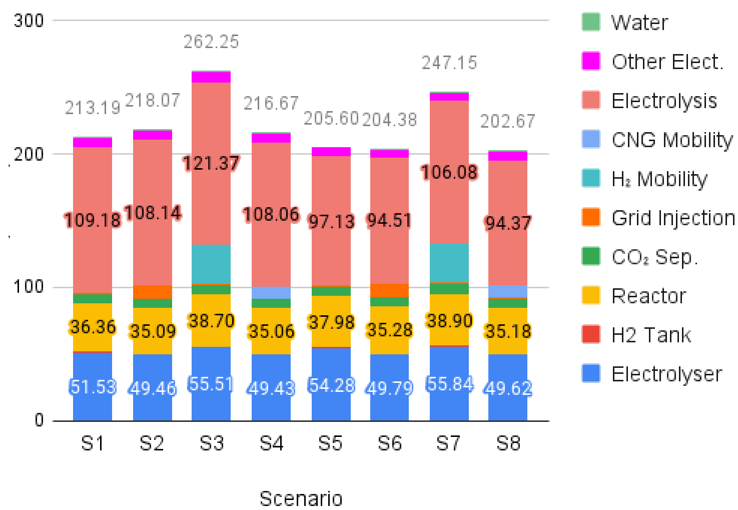


(b) LCOM grouped by equipment or electricity type.

Figure 7: Stacked column charts of the LCOM for each scenario in 2017 grouped by cost type and equipment or electricity type.

price scenarios (S5, S6 and S8). This is caused by two factors: the higher average electricity price and gas grid availability for the year.

The highest LCOM is always when $H_2$ mobility is considered (S3 and S7).

This is due to its very high capital costs, namely the refilling site and tube-trailers. However, this can be slightly misleading as the LCOM is considering the levelized costs per unit energy of methane, which would be produced less in this configuration as the $H_2$ is used for mobility instead (when producing SNG is not possible). The revenue gained from $H_2$ mobility also needs to be considered to see if the additional investment is justified.

### *3.4.2. Minimum Selling Price*

As shown in Equation 5, MSP subtracts $H_2$ mobility and FCR participation revenue from LCOM, providing the minimum price produced SNG would need to be sold at to break-even on the project. As seen in Table 12, the most favorable scenarios from LCOM analysis are also the same for MSP. It is interesting to investigate the influence the additional revenue streams have on reducing the MSP of SNG which is done by first taking the difference between LCOM and MSP and computing each revenues' portion of this LCOM reduction. This difference is shown graphically in Figure 8 with each revenue type highlighted. As one can see, the reduction in LCOM by FCR revenue is roughly the same for every scenario and year (29.73-34.20 €/MWh); this is due to electrolyser operational hours of the plant being very similar in every scenario (discussed later in section 3.4.3). As the electrolyser is participating in the FCR whenever it is operational, revenue is directly correlated to electrolyser OH (see Equation 7). When $H_2$ mobility is considered, the reduction in LCOM is almost doubled (up to 63.56 €/MWh), which only consumes about 11% of yearly $H_2$ production. This highlights the premium paid for $H_2$ in mobility applications and its reason for being the main application of renewable $H_2$ production. However, the MSP in $H_2$ mobility scenarios

(S3 and S7) are still higher than all other scenarios despite this doubling in LCOM reduction. This can be attributed to the high CAPEX associated to $H_2$ mobility (discussed in section 3.4.5).

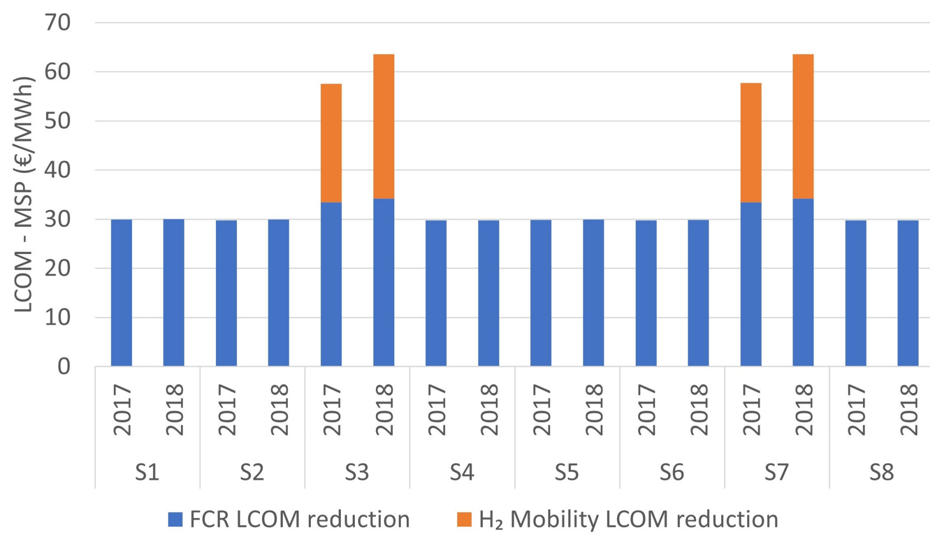


Figure 8: Difference between LCOM and MSP broken down by revenue type for each scenario and year.

Selling prices of 172.91-204.73 €/MWh for produced SNG are high when compared to the wholesale price of NG on the spot market at around 20 €/MWh [45]. Bio-NG is currently sold and injected into the French NG grid via fixed tariffs between the producer and gas supplier for a fixed term at a price between 45-139 €/MWh depending upon the biogas source and production capacity [24]. However, as per the multiannual energy programming (PPE), these tariffs are to be reduced to a target price of 75 €/MWh by 2023 and 60 €/MWh by 2028 [46]. SNG is currently not given any government support as it is a relatively new product which has been implemented in only 3 projects in France at the time of writing with power ratings no greater than

1 MW [3]. The results presented clearly show a necessity for SNG to receive a similar tariff scheme as bio-NG, with arguably higher rates. Depending on plant configuration, Bio-NG production may only require biogas upgrading equipment while SNG production requires costly $H_2$ and $CH_4$ conversion equipment, numerous gas storage mediums and $CO_2$ capture and possibly purification technology.

FCR participation as a secondary revenue stream is very attractive, especially when using the innovative electrolyser technology allowing 200% rated capacity operation for short durations, allowing no sacrifice on rated capacity to normal operation. It provided a 29.73-34.20 €/MWh or 13.6-24% reduction in LCOM, significantly impacting the MSP of SNG.

### *3.4.3. Yearly Operational Hours*

Electrolyser OH ($OH_{elect}$) is high for all scenarios, between 7,587 and 8,322 as shown in Table 12. A fixed electricity price (S1-S4) allows electrolyser production to only be limited by tank capacity while the high $WTP_{det}$ of 95 €/MWh used in DA price scenarios (S5-S8) hardly limits production. This can be seen especially if looking at the scenarios with the lowest OH: NG injection only (S1 and S5). $OH_{elect}$ and $OH_{rea}$ are shown in Table 13 and a count of the hours maximum tank capacity ($tank_{cap}$) stopped electrolyser production and grid injection capacity ($grid_{cap}$) prohibited reactor operation. As hydrogen storage is considered in the plant, operation of the electrolyser and reactor are decoupled and thus these restrictions only limit the directly affected component. As electricity price is not a constraint in S1, the summation of $OH_{elect}$ and $tank_{cap}$ equals the total hours in a year (8760) as does $OH_{rea}$ and $grid_{cap}$. However, in S5, the additional constraint of $WTP_{det}$ =

95 €/MWh reduces $OH_{elect}$ by about 300-500 hours per year. This reduction has a ripple effect on reactor operation due to the small tank sizes.

Table 13: Operational hours of electrolyser and reactor for the NG injection scenarios (S1 and S5) in each year, showing their limitations and portion of wind power.

| Scenario | Year | $\mathbf{OH_{elect}}$ | $\mathbf{Tank_{cap}}$ | $\mathbf{OH_{rea}}$ | $\mathbf{Grid_{cap}}$ | $\mathbf{OH_{elect,wind}}$ |
|---|---|---|---|---|---|---|
| S1 | 2017 | 8,031 | 728 | 7,831 | 929 | 6065 |
| | 2018 | 8,035 | 725 | 7,655 | 1,105 | 6,110 |
| S5 | 2017 | 7,587 | 699 | 7,384 | 929 | 5,790 |
| | 2018 | 7,767 | 683 | 7,425 | 1,105 | 6,267 |

A general trend of lower OH can be seen in scenarios using the DA market prices, attributed to the more flexible operation to take advantage of lower electricity prices. One final point is the amount of $OH_{elect}$ which virtually followed the wind power profile, as shown in Table 13: 75-81% of the presented scenarios electrolyser consumed power. The other scenarios fall in this same range, showing a high majority of renewable power used for $H_2$ production.

### *3.4.4. Tank Size*

Tank sizes were optimized for each scenario in terms of minimizing LCOM and are shown in Table 12. The same sizes were used in both years to compare its effect in each year and simplify modeling. The largest size is found in S5 (NG injection only) which is equal about 1.5 hours of electrolyser operation, meaning longer storage of days or seasonally is not economically attractive for this project. This is largely based upon the high grid injection availability year-round. Further, the mobility scenarios have minimal storage due to their independent higher pressure storage on-site of their respective stations.

### 3.4.5. CAPEX

The CAPEX of all scenarios for both years are the same as the equipment does not change. As stated previously, S2-S4 and S6-S8 have equipment which is added to S1 and S5, respectively, to increase SNG production, meaning a higher CAPEX. As would be expected, the standard configuration (S1) has the lowest CAPEX due to its limited amount of equipment compared to other scenarios. The $H_2$ mobility scenarios (S3 and S7) have the highest CAPEX due to the current high capital cost of equipment required, namely the tube-trailers, refilling site and compressor.

### 3.4.6. Key Metric Spider Chart Comparison

A scaled visual comparison of the key metrics can be done using Equations 9 and 10. For the operational metrics – $OH_{elect}$ and $H_2$ tank size – the largest value was ranked the highest whereas the economical metrics – LCOM, MSP and CAPEX – the lowest value was ranked the highest. Using a range $= [0, 5]$, the spider charts shown in Figure 9 were generated showing the scaled values of the metrics for each scenario and year.

Using this figure and the previous sections, the most interesting scenarios for this project are S5 and S8 – using variable DA market electricity prices with either the standard configuration or including a CNG mobility station on-site. It should be noted that the difference in input data for each year caused considerable changes in each scenario's LCOM and MSP - the most important metrics to consider for project feasibility studies.

It should be noted that CNG mobility being one of the best configura-

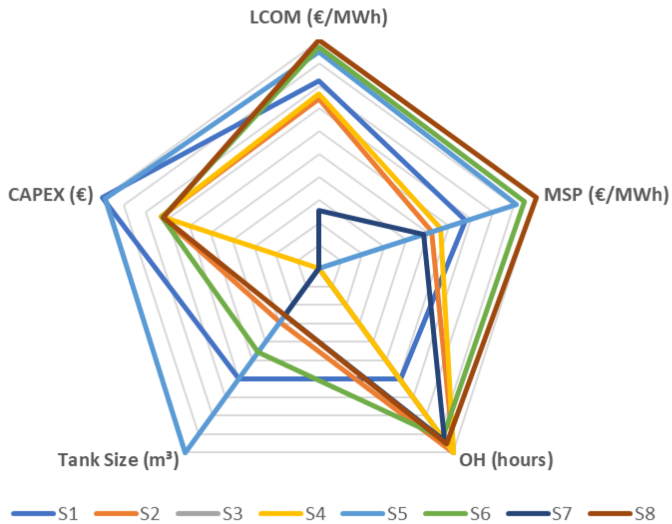


(a) 2017

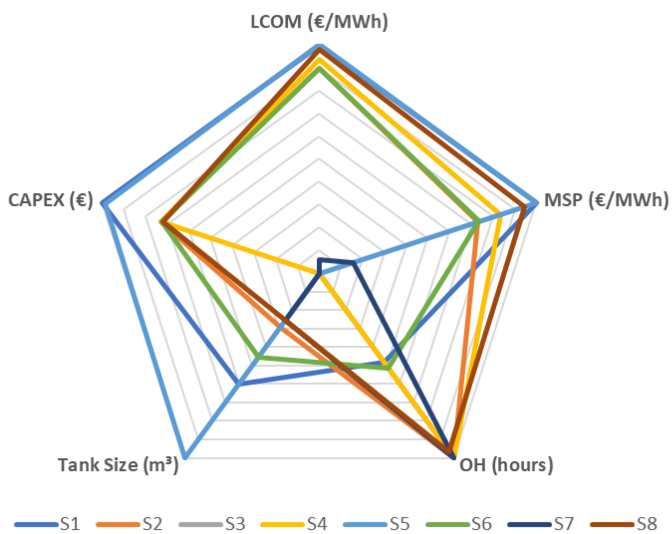


(b) 2018

Figure 9: Spider charts of the key metrics for each year.

tions should be taken with caution. For modeling purposes, a continuous flow rate of SNG is sent to the station equal to two waste trucks' yearly consumption. Further, extra SNG production not accepted by the grid is sent to the station, which is assumed to be consumed in some fashion by increased truck consumption. This volatility in consumption, portrayed very favorably in modeling, does not provide guaranteed revenue like grid injection would in real-world applications. In addition, CNG mobility stations are normally connected to the gas grid instead of directly to production sites as modeled here; this presents uncertainty in tariffs being applied to SNG sold for mobility in this configuration.

The attractiveness of hydrogen mobility could be seen in the results presented, as other sources have also confirmed as currently the best market for power-to-gas [20, 17, 19]. However, the plant studied used mobility as a secondary application to SNG grid injection, which did not provide enough hydrogen production to be sold to mobility distributors for sufficient returns on the high equipment cost. An alternative plant configuration would be to have $H_2$ mobility as the primary application, with grid injection - preferably pure $H_2$ if the local grid distribution network allows it - as the secondary application. Indeed, this type of configuration was studied by [20] which also considered it an attractive topology.

### *3.5. Sensitivity Analysis*

A sensitivity analysis of the most influential factors for S5 and S8 is done to see their effect on MSP. The electricity price, gas grid availability, electrolyser efficiency and electrolyser and reactor CAPEX are modified by ±20%. The data of year 2017 is used due to its better performance in the original analysis. The results are shown in Figure 10.

The most influential factor is electrolyser efficiency, which is able to reduce the MSP by 21-24 €/MWh for a minimum of 149.01 €/MWh, due to the

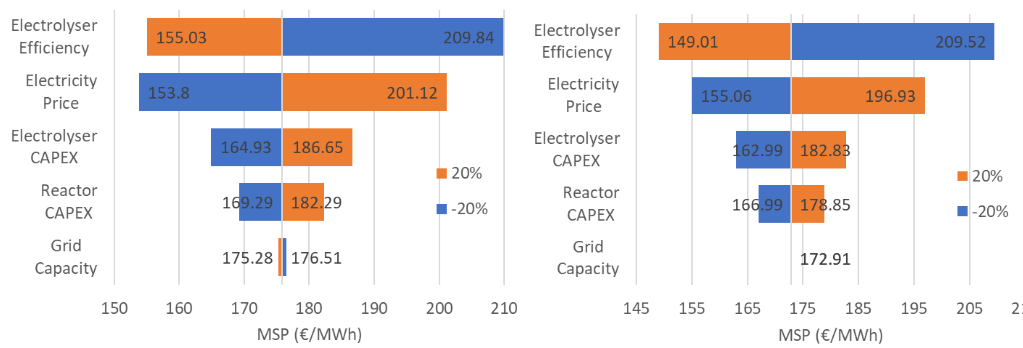


(a) S5 - standard configuration with DA electricity. (b) S8 - CNG mobility with DA electricity.

Figure 10: Tornado charts of S5 and S8 for 2017 showing a ±20% sensitivity analysis on MSP.

reduced electricity consumption and thus electricity cost. In contrast, it is also capable of greatly increasing the MSP if the efficiency were to decrease. Electricity price is a close second in its impact on MSP, giving the lowest results in S5 at 153.80 €/MWh and an overall 18-22 €/MWh reduction. The electrolyser and reactor CAPEX are the next most influential, respectively, with their impact less than 50% of that done by electricity price. Referencing Figure 7a showing the total CAPEX portion on scenario LCOM, this relative impact is to be expected. Grid capacity has extremely little impact on S5 and no impact at all on S8. For S5, this negligible impact is mainly due to the already high availability of grid injection and variability in times of no availability: there is almost never long durations in limited grid availability that would greatly effect production. S5 has 6.5 hours of intermediate $H_2$ storage that seems to be able to allow production to continue with reduced grid consumption as per the sensitivity analysis. No impact on S8 is due to the plant's ability to direct the SNG production to CNG mobility when there is no grid availability.

The sensitivity analysis clearly shows the impact of improved electrolyser efficiency on a PtG plant's profitability. The electrolyser efficiency used is approximately 71% $\left(\frac{5kWh/Nm^3}{3.54kWh/Nm^3\,HHV} = 0.71\right)$, meaning efficiency would need to increase to 90% to get similar results as shown. Studies show efficiencies of 83% are projected by mid-decade and possibly up to 90% by 2030, suggesting these results could be possible when commercial plants are being deployed [47]. The presented CAPEX reduction is projected to be significantly surpassed with projections as low as 250 €/kW$_{\mathrm{el}}$ by 2030 for PEM electrolysers [47] and 500 €/kW$_{\mathrm{el}}$ for biological reactors [3]. In general, electricity prices are projected to increase as the share of renewables increases in power production, with lower variability in the year due to lower marginal costs [48]. This will mean government support for PtG plants in forms of tax exemptions or other schemes is needed to reduce the primary production cost until CAPEX's or electrolyser efficiency improve.

## 4. Conclusion and Future Work

This paper has described a modeling methodology for analysing PtG plants with a special focus on unique local conditions, limitations and opportunities for the purpose of performing a feasibility analysis for projects. It has shown that these parameters can greatly influence production costs and minimum selling price of product gases, namely synthetic natural gas for the pilot project presented as a case study. Most importantly, the analysis showed that the cost of production is still too high for synthetic natural gas to compete with not only natural gas but biomethane. The current support structure for biomethane in France allows operators to receive a fixed price for production, giving security to their investment. Similar regulation must be put in place for synthetic natural gas, as well as hydrogen grid injection, if France hopes to build up the renewable gas market domestically. These regulations can highlight that power-to-gas plants are not only producing lower emission gases but can also reduce variable renewable energy penetration, if built in strategic locations. In terms of HYCAUNAIS, carbon emissions from the landfill is being reduced as much as possible while maximising methane production, which seeks to benefit all involved.

Another positive from power-to-gas facilities is the multiple end-use applications of the product gases. As seen in this analysis, mobility and gas grid injection could both be applied to the plant, provided the additional operational hours and cost don't result in higher levelized costs. Although hydrogen mobility is known to have higher capital costs, this could be outweighed by the premium price paid at the pump. Primary applications of the plant must be holistically considered to ensure profit maximisation occurs, meaning the main end-use application of the plant should be considered with all local conditions and market values known. A market which was shown to help improve the economics was electricity ancillary services. This added revenue stream could be done without sacrificing production because of an innovative electrolyser design allowing 200% maximum capacity for short durations. If these types of electrolysers were deployed and accepted by regulators for market participation, they can greatly improve power-to-gas business cases.

In conclusion, what the analysis has shown is the importance of a qualitative survey of a project's local surroundings. What has been seen in literature to-date are generic analyses of either national power-to-gas potential or plant installation without a full consideration of local limitations or opportunities, such as: natural gas grid availability, all possible gas markets or electricity prices. Individually, these parameters can have profound implications on operational strategy; together they can completely change the plant's operational objective and its feasibility. Meeting climate targets for emission reductions and renewable energy cannot be realized without the help of technologies such as power-to-gas and these technologies cannot be implemented without complex, holistic feasibility analyses.


## Funding

This research was supported by the HYCAUNAIS project (agreement number 1882C0096) with financial support provided by the Agency of Ecological Transition in France (ADEME) under the "Investissements d'Avenir de l'Etat" aid programme, the EIPHI Graduate School (contract number ANR-17-EURE-0002) and the Region Bourgogne Franche-Comté and Bpifrance under "fond régional d'investissement" (FRI).


## References


[1] European Commission, 2030 climate & energy framework, URL: https://ec.europa.eu/clima/policies/strategies/2030_en#tab-0-0 (2014).

[2] H. Kondziella, T. Bruckner, Flexibility requirements of renewable energy based electricity systems – a review of research results and

methodologies, Renewable and Sustainable Energy Reviews 53 (2016) 10 – 22. doi:https://doi.org/10.1016/j.rser.2015.07.199.
URL http://www.sciencedirect.com/science/article/pii/S1364032115008643

[3] M. Thema, F. Bauer, M. Sterner, Power-to-Gas: Electrolysis and methanation status review, Renewable and Sustainable Energy Reviews 112 (2019) 775 – 787. doi:https://doi.org/10.1016/j.rser.2019.06.030.
URL http://www.sciencedirect.com/science/article/pii/S136403211930423X

[4] A. Boubenia, A. Hafaifa, A. Kouzou, M. Becherif, Techno economic assessment of hybrid renewable energy systems based on power to hydrogen and methane gas concepts, Preprints (2018). doi:10.20944/preprints201809.0023.v1.

[5] A. Lewandowska-Bernat, U. Desideri, Opportunities of power-to-gas technology in different energy systems architectures, Applied Energy 228 (2018) 57–67. doi:https://doi.org/10.1016/j.apenergy.2018.06.001.
URL https://www.sciencedirect.com/science/article/pii/S0306261918308675

[6] M. Qadrdan, M. Abeysekera, M. Chaudry, J. Wu, N. Jenkins, Role of power-to-gas in an integrated gas and electricity system in great britain, International Journal of Hydrogen Energy 40 (17) (2015) 5763 – 5775. doi:https://doi.org/10.1016/j.ijhydene.2015.03.004.
URL http://www.sciencedirect.com/science/article/pii/S0360319915005418

[7] J. Burkhardt, A. Patyk, P. Tanguy, C. Retzke, Hydrogen mobility from wind energy – a life cycle assessment focusing on the fuel supply, Applied Energy 181 (2016) 54–64. doi:https://doi.org/10.1016/j.apenergy.2016.07.104.
URL `https://www.sciencedirect.com/science/article/pii/S0306261916310492`

[8] IEA, The Future of Hydrogen – Analysis (Jun. 2019).
URL `https://www.iea.org/reports/the-future-of-hydrogen`

[9] R. McKenna, Q. Bchini, J. Weinand, J. Michaelis, S. König, W. Köppel, W. Fichtner, The future role of power-to-gas in the energy transition: Regional and local techno-economic analyses in baden-württemberg, Applied Energy 212 (2018) 386–400. doi:https://doi.org/10.1016/j.apenergy.2017.12.017.
URL `https://www.sciencedirect.com/science/article/pii/S0306261917317312`

[10] C. Wulf, P. Zapp, A. Schreiber, Review of Power-to-X Demonstration Projects in Europe, Frontiers in Energy Research 8 (2020) 191. doi:10.3389/fenrg.2020.00191.
URL `https://www.frontiersin.org/article/10.3389/fenrg.2020.00191`

[11] M. Götz, J. Lefebvre, F. Mörs, A. McDaniel Koch, F. Graf, S. Bajohr, R. Reimert, T. Kolb, Renewable Power-to-Gas: A technological and economic review, Renewable Energy 85 (2016) 1371 – 1390. doi:https://doi.org/10.1016/j.renene.2015.07.066.

URL http://www.sciencedirect.com/science/article/pii/S0960148115301610

[12] European Network of Transmission System Operators for Gas, System Development Map, https://entsog.eu/sites/default/files/2021-01/ENTSOG_GIE_SYSDEV_2019-2020_1600x1200_FULL_047.pdf, brussels (2020).

[13] P. D. Lund, J. Lindgren, J. Mikkola, J. Salpakari, Review of energy system flexibility measures to enable high levels of variable renewable electricity, Renewable and Sustainable Energy Reviews 45 (2015) 785 – 807. doi:https://doi.org/10.1016/j.rser.2015.01.057.
URL http://www.sciencedirect.com/science/article/pii/S1364032115000672

[14] C. Wulf, J. Linßen, P. Zapp, Review of Power-to-Gas Projects in Europe, Energy Procedia 155 (2018) 367 – 378, 12th International Renewable Energy Storage Conference, IRES 2018, 13-15 March 2018, Düsseldorf, Germany. doi:https://doi.org/10.1016/j.egypro.2018.11.041.
URL http://www.sciencedirect.com/science/article/pii/S1876610218309883

[15] C. van Leeuwen, A. Zauner, Report on the costs involved with PtG technologies and their potentials across the EU (D8.3), sTORE&GO Project (2018).

[16] D. Hissel, Hydrogen economy: myth or reality?, in: International Smart

Grid Conference, Paris, France, 2020.
URL https://hal.archives-ouvertes.fr/hal-02993911

[17] J. de Bucy, O. Lacroix, The Potential of Power-to-Gas, Tech. rep., ENEA Consulting, Paris (2016).

[18] S. McDonagh, R. O'Shea, D. M. Wall, J. Deane, J. D. Murphy, Modelling of a power-to-gas system to predict the levelised cost of energy of an advanced renewable gaseous transport fuel, Applied Energy 215 (2018) 444–456. doi:https://doi.org/10.1016/j.apenergy.2018.02.019.
URL https://www.sciencedirect.com/science/article/pii/S0306261918301387

[19] C. Breyer, E. Tsupari, V. Tikka, P. Vainikka, Power-to-gas as an emerging profitable business through creating an integrated value chain, Energy Procedia 73 (2015) 182 – 189, 9th International Renewable Energy Storage Conference, IRES 2015. doi:https://doi.org/10.1016/j.egypro.2015.07.668.
URL http://www.sciencedirect.com/science/article/pii/S1876610215014368

[20] Tractebel, Hinicio, Study on early business cases for hydrogen in energy storage and more broadly power to hydrogen applications, Tech. rep., Fuel Cells and Hydrogen 2 Joint Undertaking (2017).

[21] J. Gorre, F. Ortloff, C. van Leeuwen, Production costs for synthetic methane in 2030 and 2050 of an optimized power-to-gas plant with intermediate hydrogen storage, Applied Energy 253 (2019) 113594.

doi:https://doi.org/10.1016/j.apenergy.2019.113594.
URL http://www.sciencedirect.com/science/article/pii/S0306261919312681

[22] Agence de la transition écologique, HYCAUNAIS V2, https://www.ademe.fr/hycaunais-v2 (2019).

[23] Waga Energy, Technology: WAGABOX, an innovative landfill gas recovery solution, URL: https://waga-energy.com/en/technology/ (2020).

[24] GRDF, GRTgaz, SPEGNN, SER, Teréga, Panorama du gaz renouvelable en 2019 (2019).

[25] IEA, An introduction to biogas and biomethane – Outlook for biogas and biomethane: Prospects for organic growth – Analysis (2020).
URL https://www.iea.org/reports/outlook-for-biogas-and-biomethane-prospects-f
an-introduction-to-biogas-and-biomethane

[26] A. Buttler, H. Spliethoff, Current status of water electrolysis for energy storage, grid balancing and sector coupling via power-to-gas and power-to-liquids: A review, Renewable and Sustainable Energy Reviews 82 (2018) 2440 – 2454. doi:https://doi.org/10.1016/j.rser.2017.09.003.
URL http://www.sciencedirect.com/science/article/pii/S136403211731242X

[27] RTE, Règles Services Système Fréquence, https://www.services-rte.com/files/live/sites/services-rte/files/pdf/

Service\%20systemes\%20frequence/20181026_Regles_services_systeme_frequence.pdf (2018).

[28] B. Guinot, F. Montignac, B. Champel, D. Vannucci, Profitability of an electrolysis based hydrogen production plant providing grid balancing services, International Journal of Hydrogen Energy 40 (29) (2015) 8778 – 8787. doi:https://doi.org/10.1016/j.ijhydene.2015.05.033.
URL http://www.sciencedirect.com/science/article/pii/S0360319915011775

[29] M. Lehner, R. Tichler, H. Steinmuller, M. Koppe, Power-to-Gas: Technology and Business Models, Springer, 2014.

[30] B. Lecker, L. Illi, A. Lemmer, H. Oechsner, Biological hydrogen methanation – a review, Bioresource Technology 245 (2017) 1220 – 1228. doi:https://doi.org/10.1016/j.biortech.2017.08.176.
URL http://www.sciencedirect.com/science/article/pii/S0960852417314906

[31] J. Gorre, F. Ruoss, H. Karjunen, J. Schaffert, T. Tynjälä, Cost benefits of optimizing hydrogen storage and methanation capacities for Power-to-Gas plants in dynamic operation, Applied Energy 257 (2020) 113967. doi:https://doi.org/10.1016/j.apenergy.2019.113967.
URL http://www.sciencedirect.com/science/article/pii/S030626191931654X

[32] Electrochaea, Power-to-Gas via Biological Catalysis (P2G-Biocat) - Final Report, Tech. rep., Electrochaea, Denmark (2017).

[33] F. Bauer, T. Persson, C. Hulteberg, D. Tamm, Biogas upgrading – review of commercial technologies, Tech. rep., Swedish Gas Technology Centre, Malmö (2013).

[34] P. Collet, E. Flottes, A. Favre, L. Raynal, H. Pierre, S. Capela, C. Peregrina, Techno-economic and Life Cycle Assessment of methane production via biogas upgrading and power to gas technology, Applied Energy 192 (2017) 282 – 295. doi:https://doi.org/10.1016/j.apenergy.2016.08.181.
URL http://www.sciencedirect.com/science/article/pii/S0306261916312909

[35] J. Pépinot, Transport: Les bus à hydrogène de l'Auxerrois mis en service le 1er janvier 2021 pour les voyageurs, URL: https://www.lyonne.fr/auxerre-89000/actualites/les-bus-a-hydrogene-de-l-auxerrois-mis-en-service-le-1er-janvier-2021-pour-le
13655307/ (2019).

[36] M. Smith, J. Gonzales, Costs Associated With Compressed Natural Gas Vehicle Fueling Infrastructure, Tech. rep., National Renewable Energy Lab (9 2014). doi:10.2172/1156975.

[37] J. André, S. Auray, D. De Wolf, M.-M. Memmah, A. Simonnet, Time development of new hydrogen transmission pipeline networks for France, International Journal of Hydrogen Energy 39 (20) (2014) 10323 – 10337. doi:https://doi.org/10.1016/j.ijhydene.2014.04.190.
URL http://www.sciencedirect.com/science/article/pii/S0360319914012804

[38] W. Mallon, L. Buit, J. van Wingerden, H. Lemmens, N. H. Eldrup, Costs of $CO_2$ Transportation Infrastructures, Energy Procedia 37 (2013) 2969 – 2980, gHGT-11 Proceedings of the 11th International Conference on Greenhouse Gas Control Technologies, 18-22 November 2012, Kyoto, Japan. doi:https://doi.org/10.1016/j.egypro.2013.06.183. URL http://www.sciencedirect.com/science/article/pii/S1876610213004268

[39] IEA, Countries: France, International Energy Agency, URL: https://www.iea.org/countries/France (2020).

[40] C. van Leeuwen, M. Mulder, Power-to-gas in electricity markets dominated by renewables, Applied Energy 232 (2018) 258 – 272. doi:https://doi.org/10.1016/j.apenergy.2018.09.217. URL http://www.sciencedirect.com/science/article/pii/S0306261918315319

[41] RTE, Frequency Ancillary Services Terms and Conditions, https://www.services-rte.com/files/live/sites/services-rte/files/pdf/Service\%20systemes\%20frequence/SSY_20200530_EN.pdf (2020).

[42] A. Burke, H. Zhao, Fuel Economy Analysis of Medium/Heavy-duty Trucks – 2015-2050, EVS30 Symposium (10 2017).

[43] IBNet Tariffs DB, Ville de Strasbourg Water Dept(France), URL: https://tariffs.ib-net.org/sites/IBNET/ViewTariff?tariffId=18137&countryId=0 (2020).

[44] RTE, Portail Clients – Réserve contractualisée d'ajustement, URL: https://clients.rte-france.com/lang/fr/visiteurs/vie/reserve_ajustement.jsp (2020).

[45] EEX, EEX: Natural gas markets, URL: https://www.powernext.com/natural-gas-trading (2020).

[46] M. Lemonde, What is the State of Biogas and Biomethane Market in France?, Biogas World, URL: https://www.biogasworld.com/news/biogas-biomethane-market-france/ (2020).

[47] L. Bertuccioli, A. Chan, D. Hart, F. Lehner, B. Madden, E. Standen, Study on development of water electrolysis in the EU, Tech. rep., E4tech Sarl and Element Energy Ltd (2014).

[48] DNV GL, Imperial College London, NERA Economic Consulting, Integration of Renewable Energy in Europe, https://ec.europa.eu/energy/sites/ener/files/documents/201406_report_renewables_integration_europe.pdf (2014).